Feasibility Study of Multi-Wavelength Optical Probe to Analyze Magnesium Implant Degradation Effects

Hafiz Wajahat Hassan
Department of MEK
OsloMet - Oslo Metropolitan University
Oslo, Norway
wajahath@oslomet.no

Anna Mathew
Department of MEK
OsloMet- Oslo Metropolitan University
Oslo, Norway
annamathew17@gmail.com

Haroon Khan
Department of MEK
OsloMet - Oslo Metropolitan University
Oslo, Norway
haroonkh@oslomet.no

Olga Korostynska
Department of MEK
OsloMet - Oslo Metropolitan University
Oslo, Norway
olga.korostynska@oslomet.no

Peyman Mirtaheri*
Department of MEK
OsloMet - Oslo Metropolitan University
Oslo, Norway
peymanm@oslomet.no

***Abstract*—Near-infrared spectroscopy (NIRS) is a rapidly developing and promising technology with potential for spectrographic analysis. Understanding NIRS measurements on the implant-tissue interface for hydrogen gas formation as part of degradation is essential for interpreting the biodegradable Magnesium (Mg) based implants. This paper introduces novel NIR optical probe that can assess the state of Mg implant's degradation when in contact with biological tissues. A tissue-mimicking phantom (TMP) to mimic biological tissue's optical properties helps investigate changes in reflectance spectra due to bubble formation at the implant-tissue interface. Spectra taken from different TMP samples containing biodegradable Mg and non-degradable Titanium (Ti) disk are suitable for evaluating the implant's interaction. The results show that the reflection in TMP for samples containing Mg disks, confirms the presence of hydrogen bubbles at the surface of implants. Multi-distance optical probe with depth selectivity of 3mm and 4mm has shown to be an effective tool to monitor bubble effect on different samples.**

***Index Terms*—Optical probe, Near-infrared spectroscopy (NIRS), Biodegradable Magnesium (Mg) implants, Tissue diagnostics**

I. Introduction

In recent decades, magnesium (Mg) and its alloys have been widely explored due to their features that make these materials attractive candidates for biodegradable materials in medical applications [1, 2]. In addition, these materials are biocompatible and possess mechanical qualities suitable for orthopaedic implants [3, 4]. During the Mg implant's degradation in vivo, the hydrogen gas cavity is produced. Literature confirms that gas cavities are usually perforated subcutaneously in numerous animal model-based experiments, which needs monitoring as part of evaluating the progress of implant [5].

Near-infrared spectroscopy (NIRS) has been developed over four decades ago [6] and is now conventional tissue-blood oxygenation measuring technology to measure oxygenation haemoglobin (HbO), deoxygenation haemoglobin (HbR), and oxygen (O_2) saturation [7]. The potential of NIRS for bioprocess monitoring, where a range of analytes can be measured in real-time, has been investigated [8]. Such measures can be beneficial for several applications and automatic control. However, the success of NIRS for bioprocess monitoring is still not a routine, because bioprocessing possess various challenges. One of them is the biodegradation of Mg, which exhibits gas formation upon implantation [9]. There are many technologies to measure the Mg degradation and its effects including computed tomography (CT) [10], synchrotron-radiation-based computer microtomography (SRμCT) [11], positron emission tomography (PET) [12], magnetic resonance imaging (MRI) [13], and ultrasound photoacoustic (USPA) [14]. However, the bubble formation needs to be investigated extensively. For that reason, NIRS is a potential candidate, and its feasibility has been discussed in a recently published comprehensive review [15].

In this paper, a novel multi-distance NIRS optical probe that can be used to investigate the bubble formation and its effect due to the Mg implant is proposed. Furthermore, a comparison of reflectance graphs at two different depths was evaluated.

II. Material and Methods

In this pilot study, a total of 3 Mg alloy (ZX00) disks with $0.45\ wt\ \%\ Zn - 0.45\ wt\ \%\ Ca$ from BRI.Tech (Austria) were used. Different disks were used for comparison containing Mg alloy, control (no disk in phantom), and pure Ti disks. Two disks were placed in Dulbecco's modified eagle medium (DMEM) solution for ten days out of three Mg

This publication is part of a project "Promoting patient safety by a novel combination of imaging technologies for biodegradable magnesium implants, MgSafe " that has received funding from the European Union's Horizon 2020 research and innovation program under the Marie Skłodowska-Curie grant agreement No 811226.

*Corresponding author: Peymanm@oslomet.no

disks. An incubator (TS8056, Termaks) at 37° C with 5% carbon dioxide CO_2 with 21% O_2 was used [16]. One of the disk's surfaces was damaged from the sandpaper to get the roughness properties of the material surface. The effect of bubble formation and optical properties in the medium was investigated based on a TMP mimicking the breast tissue [17].

A. Tissue-mimicking Phantom (TMP)

The development of most physical therapeutic and diagnostic imaging systems requires tissue phantoms that exhibit human or animal tissue qualities. For several reasons, the usage of so-called "phantoms", includes initial testing of system designs and comparison [18, 19]. For TMP formation, a gelatine substrate was used as the base structure, while titanium dioxide TiO_2 was applied as scattering particles, India ink was used as an absorber and ethylenediaminetetraacetic acid (EDTA) solution was used to avoid bacterial infection. In addition to the above procedure, 0.2 % Formaldehyde was added in the solution to work with the TMP at room temperature [18]. The concentration of India ink was within the range of 0.002-0.0012 mm^{-1} and TiO_2 was selected 0.4 mm^{-1} at 1 g/L that is less than 0.5-1.3 mm^{-1}, and for normally found in human breast tissue [17, 20].

B. Multi-wavelength Optical Probe

An application-specific probe was designed at the Optical NIRS lab facility in OsloMet - Oslo Metropolitan university to investigate Mg implant's degradation process in tissues. The optical probe used in this experiment contains two identical broadband light sources (SFH4735, Osram, Germany) which works within the NIR range from 600 to 1050 nm. Because of the non-ionizing nature of NIR light, it does not change genetic information, unlike ultraviolet radiations, which may cause problems like tissue heating and burning due to light sources. The maximum allowed NIR lights exposure for the skin varies from 0.2 W/cm^2 in 630 nm to 0.4 W/cm^2 in 850 nm [21]. The designed optical probe's light sources are strictly compliant with this threshold to ensure the operation safety.

Avantes spectrometer (Avaspec-2048x14, Avantes, The Netherlands) is used to collect the spectrum through a detector fiber of 1000 µm. The design of the optical probe-target different sets of the region of interest (ROIs) simultaneously. Matlab ® (R2020a) was used for programming and control the switching of light sources. One of the advantages of the optical probe is to have multiple acquisitions within minutes. An illustration of the optical probe setup is shown in Fig. 1, where S is the light source, and D stands for the detector.

III. Depth Variation and Reflectance Spectra

Penetration depth can be distinguished by examining the distance traveled by the photon from the source to the detector. The depth of NIR light penetration is approximately half of the physical distance of the source-detector [22]. The source-detector distance from S_1 to D was 6 mm, and S_2 to D was 8 mm to achieve the depth of 3 mm and 4 mm, respectively. The spectrum of reflected light was measured for each sample.

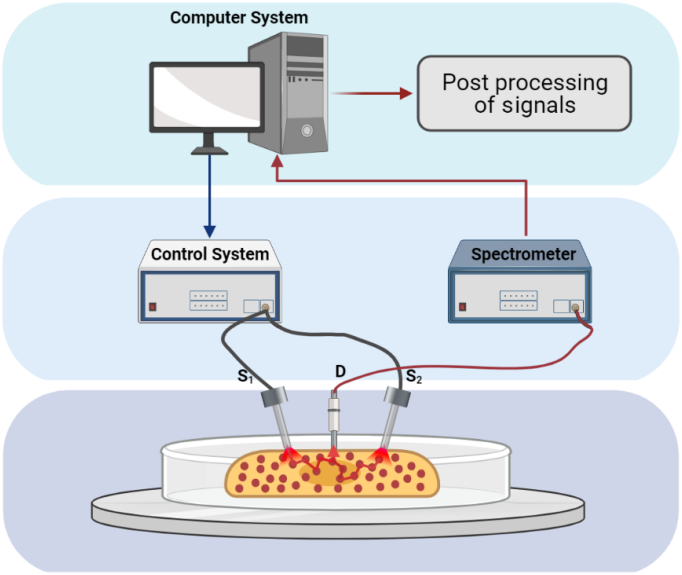

Fig. 1. Illustration of optical probe setup

All measured spectra were recorded by removing the dark reference. A white reference was utilized to standardize spectra from non-uniformities of all components of the equipment (light source, spectrometer, and optical fiber). As the optical probe is working in the reflectance mode, the calculations for reflectance at pixel "n" using the current, dark, and reference sets is determined by the following equation:

$$R_n = 100 \times \left(\frac{sample_n - dark_n}{ref_n - dark_n} \right) \quad (1)$$

NIRS data obtained with the optical probe from turbid media can be used to accurately model NIR light propagation by using modified Beer-Lambert law (MBLL). MBLL can be utilized for NIR spectroscopic investigation to quantify the variation in tissue chromophore's concentration. The MBLL explores the optical attenuation using the differential path-length factor (DPF) in highly scattering media. The DPF is a scaling factor based on wavelengths and describes how long NIRS light traveled through the media from source to detector [23]. In order to investigate the area surrounding the implant, MBLL can be used to measure the changes in concentration of different chromophores i.e, HbO, HbR and cytochrome c oxidase.

IV. Results and Discussion

Optical scattering is usually classified by the ratio of spherical particle radius to a light wavelength between Rayleigh or Mie scattering [24]. The Rayleigh scattering occurs in all directions when the size of the particle exceeds light wavelength. In contrast, the incident light is scattered mainly in the forward direction in the Mie scattering system, which corresponds with when the particle size comparable with the light wavelength. Bubble formation is observed when the disks were placed in the gel phantom. As shown in Fig. 2, the scattering is in the forward direction due to bubbles around the

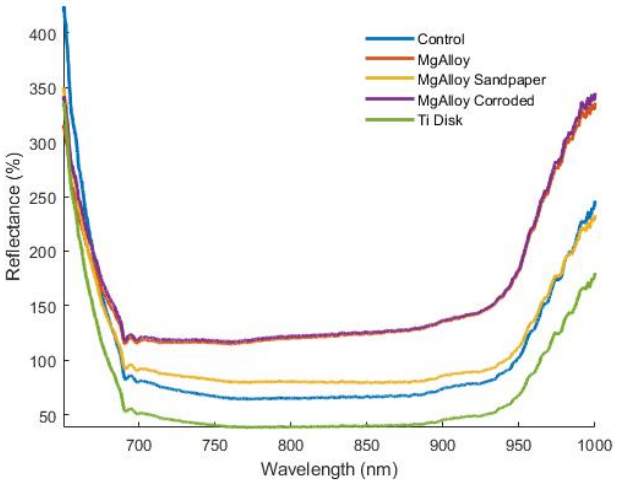

Fig. 2. Reflectance spectra from gel phantoms (4 mm depth)

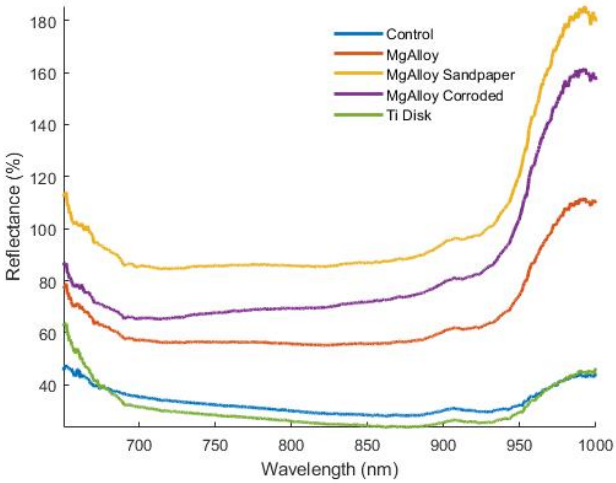

Fig. 3. Reflectance spectra from gel phantoms (3 mm depth)

tissues. The source-detector S_2-D was applied to investigate the disk-tissue interface. It was found that the Mg alloy reflection is around 60% higher as compared to Ti, corroded, and destroyed disks while calculating mean absolute error by taking control as a reference. The reason for lower spectra at the destroyed and nonhomogeneous surface is the light back-scattered due to the reflection of the Mg disk. Ti gives a similar observation because some of the light is reflected from the surface. As shown in Fig. 3, NIR light is not reaching the disk gel interface. The situation is reverted as bubbles generated by the destroyed (nonhomogeneous surface) disk are more than Mg alloy and corroded one. On the other hand, Ti and control samples have the same absorbance level because of no bubble formation, no chemical reactions as in Mg disks, and absence of back-scattered photons.

When light propagates within the tissues in the presence of air bubbles, the photons are affected mainly by Mie-scattering. While there are fewer influences from Rayleigh scattering,a forward scattering behavior is observed [25]. It may indicate a significant scattering and therefore defocusing of incident light can be minimised if air bubbles are generated along the incident path, which can boost the light penetration.

A principal component analysis (PCA) was used for analyzing the reflectance spectra. It is a statistical procedure to resolve data collection into orthogonal components whose linear combinations approach the original data to the desired precision. In terms of the product of two more minor scoring and loading matrices, PCA allows the predominant patterns to be extracted from the reflectance spectral data set matrix. Furthermore, the highly repeatable non-invasive measurements in nature help use the NIRS optical probe during and after implantation processes for tissue oxygenation. Figure 4 shows the score plot obtained from the PCA analysis (Camo, Norway), segregate effectively into two groups, the data collected from two different source-detector distances mainly 6 mm and 8 mm.

V. Conclusion

The effect of bubble formation on reflectance spectra obtained from the optical probe is studied using tissue-mimicking phantoms. Furthermore, the influence of the bubbles at the implant tissue interface due to scattering in biological tissues is comparatively analyzed using the developed optical probe and TMP. Additionally, the comparison of two different source-detector distances was separated 100% in the PCA score plot. It opens up the possibility of using the developed optical probe to differentiate the depth of NIR light in the vicinity of implant tissues interface. Hence, the feasibility studies of using a novel multi-wavelength NIR probe for Mg implant degradation showed an effective optical analysis tool.

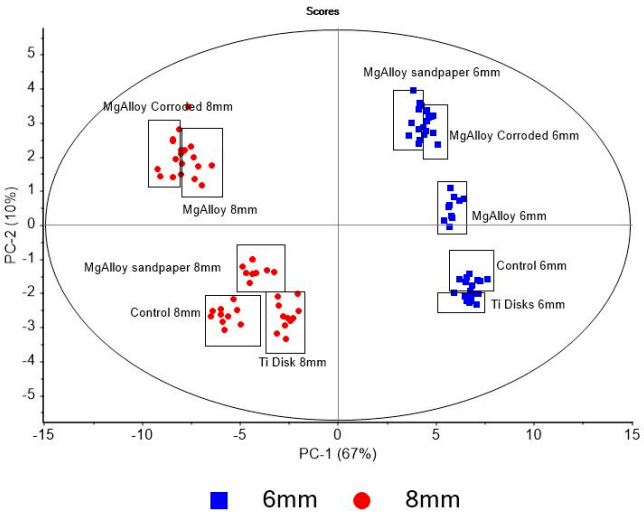

Fig. 4. Score plot from PCA

References

[1] F. Witte, V. Kaese, H. Haferkamp, E. Switzer, A. Meyer-Lindenberg, C. Wirth, and H. Windhagen, "In vivo corrosion of four magnesium alloys and the associated bone response," *Biomaterials*, vol. 26, no. 17, pp. 3557–3563, 2005.

[2] M. P. Staiger, A. M. Pietak, J. Huadmai, and G. Dias, "Magnesium and its alloys as orthopedic biomaterials: a review," *Biomaterials*, vol. 27, no. 9, pp. 1728–1734, 2006.

[3] H. Waizy, J.-M. Seitz, J. Reifenrath, A. Weizbauer, F.-W. Bach, A. Meyer-Lindenberg, B. Denkena, and H. Windhagen, "Biodegradable magnesium implants for orthopedic applications," *Journal of Materials Science*, vol. 48, no. 1, pp. 39–50, 2013.

[4] A. H. M. Sanchez, B. J. Luthringer, F. Feyerabend, and R. Willumeit, "Mg and mg alloys: how comparable are in vitro and in vivo corrosion rates? a review," *Acta biomaterialia*, vol. 13, pp. 16–31, 2015.

[5] D. Noviana, D. Paramitha, M. F. Ulum, and H. Hermawan, "The effect of hydrogen gas evolution of magnesium implant on the postimplantation mortality of rats," *Journal of Orthopaedic Translation*, vol. 5, pp. 9–15, 2016.

[6] F. F. Jobsis, "Noninvasive, infrared monitoring of cerebral and myocardial oxygen sufficiency and circulatory parameters," *Science*, vol. 198, no. 4323, pp. 1264–1267, 1977.

[7] T. Li, Y. Shang, and W. Ge, "Optical technologies for healthcare and wellness applications," 2019.

[8] A. E. Cervera, N. Petersen, A. E. Lantz, A. Larsen, and K. V. Gernaey, "Application of near-infrared spectroscopy for monitoring and control of cell culture and fermentation," *Biotechnology progress*, vol. 25, no. 6, pp. 1561–1581, 2009.

[9] Y.-K. Kim, K.-B. Lee, S.-Y. Kim, K. Bode, Y.-S. Jang, T.-Y. Kwon, M. H. Jeon, and M.-H. Lee, "Gas formation and biological effects of biodegradable magnesium in a preclinical and clinical observation," *Science and Technology of advanced MaTerialS*, vol. 19, no. 1, pp. 324–335, 2018.

[10] A. Gigante, N. Setaro, M. Rotini, S. Finzi, and M. Marinelli, "Intercondylar eminence fracture treated by resorbable magnesium screws osteosynthesis: a case series," *Injury*, vol. 49, pp. S48–S53, 2018.

[11] B. Zeller-Plumhoff, H. Helmholz, F. Feyerabend, T. Dose, F. Wilde, A. Hipp, F. Beckmann, R. Willumeit-Römer, and J. U. Hammel, "Quantitative characterization of degradation processes in situ by means of a bioreactor coupled flow chamber under physiological conditions using time-lapse srμct," *Materials and Corrosion*, vol. 69, no. 3, pp. 298–306, 2018.

[12] R. Willumeit-Römer, "The interface between degradable mg and tissue," *Jom*, vol. 71, no. 4, pp. 1447–1455, 2019.

[13] L. Sonnow, S. Könneker, P. M. Vogt, F. Wacker, and C. von Falck, "Biodegradable magnesium herbert screw–image quality and artifacts with radiography, ct and mri," *BMC medical imaging*, vol. 17, no. 1, pp. 1–9, 2017.

[14] V. Grasso, J. Holthof, and J. Jose, "An automatic unmixing approach to detect tissue chromophores from multispectral photoacoustic imaging," *Sensors*, vol. 20, no. 11, p. 3235, 2020.

[15] H. W. Hassan, V. Grasso, O. Korostynska, H. Khan, J. Jose, and P. Mirtaheri, "An overview of assessment tools for determination of biological magnesium implant degradation," *Medical Engineering & Physics*, vol. 93, pp. 49–58, 2021.

[16] I. Marco, F. Feyerabend, R. Willumeit-Römer, and O. Van der Biest, "Degradation testing of mg alloys in dulbecco's modified eagle medium: Influence of medium sterilization," *Materials Science and Engineering: C*, vol. 62, pp. 68–78, 2016.

[17] G. M. Spirou, A. A. Oraevsky, I. A. Vitkin, and W. M. Whelan, "Optical and acoustic properties at 1064 nm of polyvinyl chloride-plastisol for use as a tissue phantom in biomedical optoacoustics," *Physics in Medicine & Biology*, vol. 50, no. 14, p. N141, 2005.

[18] B. W. Pogue and M. S. Patterson, "Review of tissue simulating phantoms for optical spectroscopy, imaging and dosimetry," *Journal of biomedical optics*, vol. 11, no. 4, p. 041102, 2006.

[19] J. Olsen and E. Sager, "Subjective evaluation of image quality based on images obtained with a breast tissue phantom: comparison with a conventional image quality phantom," *The British journal of radiology*, vol. 68, no. 806, pp. 160–164, 1995.

[20] H. G. Akarçay, S. Preisser, M. Frenz, and J. Rička, "Determining the optical properties of a gelatin-tio 2 phantom at 780 nm," *Biomedical optics express*, vol. 3, no. 3, pp. 418–434, 2012.

[21] G. Strangman, D. A. Boas, and J. P. Sutton, "Non-invasive neuroimaging using near-infrared light," *Biological psychiatry*, vol. 52, no. 7, pp. 679–693, 2002.

[22] V. Quaresima and M. Ferrari, "Functional near-infrared spectroscopy (fnirs) for assessing cerebral cortex function during human behavior in natural/social situations: a concise review," *Organizational Research Methods*, vol. 22, no. 1, pp. 46–68, 2019.

[23] W. B. Baker, A. B. Parthasarathy, D. R. Busch, R. C. Mesquita, J. H. Greenberg, and A. Yodh, "Modified beer-lambert law for blood flow," *Biomedical optics express*, vol. 5, no. 11, pp. 4053–4075, 2014.

[24] X. Fan, W. Zheng, and D. J. Singh, "Light scattering and surface plasmons on small spherical particles," *Light: Science & Applications*, vol. 3, no. 6, pp. e179–e179, 2014.

[25] H. Kim and J. H. Chang, "Increased light penetration due to ultrasound-induced air bubbles in optical scattering media," *Scientific reports*, vol. 7, no. 1, pp. 1–8, 2017.